Genistein improves renal disease in a mouse model of nephropathic cystinosis: a comparison study with cysteamine

Ester De Leo[1], Anna Taranta[1], Roberto Raso[1], Elena Polishchuk[2], Valentina D'Oria[3], Marco Pezzullo[4], Bianca Maria Goffredo[5],

Sara Cairoli[5], Francesco Bellomo [iD][1], Giulia Battafarano[6], Francesca Diomedi Camassei[7], Andrea Del Fattore [iD][6], Roman Polishchuk[2],

Francesco Emma[1,8] and Laura Rita Rega [iD][1,*]

[1]Renal Diseases Research Unit, Genetics and Rare Diseases Research Area, Bambino Gesù Children's Hospital, IRCCS, 00146 Rome, Italy
[2]Telethon Institute of Genetics and Medicine, 80078 Pozzuoli, Italy
[3]Research Laboratories, Confocal Microscopy Core Facility, Bambino Gesù Children's Hospital, IRCCS, 00146 Rome, Italy
[4]Core Facilities, Bambino Gesù Children's Hospital, IRCCS, 00146 Rome, Italy
[5]Department of Pediatric Specialties and Liver-Kidney Transplantation, Division of Metabolic Biochemistry and Drug Biology, Bambino Gesù Children's Hospital, IRCCS, 00146 Rome, Italy
[6]Bone Physiopathology Research Unit, Genetics and Rare Diseases Research Division, Bambino Gesù Children's Hospital, IRCCS, 00146 Rome, Italy
[7]Department of Laboratories-Pathology Unit, Bambino Gesù Children's Hospital, 00165 Rome, Italy
[8]Division of Nephrology, Department of Pediatric Subspecialties, Bambino Gesù Children's Hospital, IRCCS, 00146 Rome, Italy
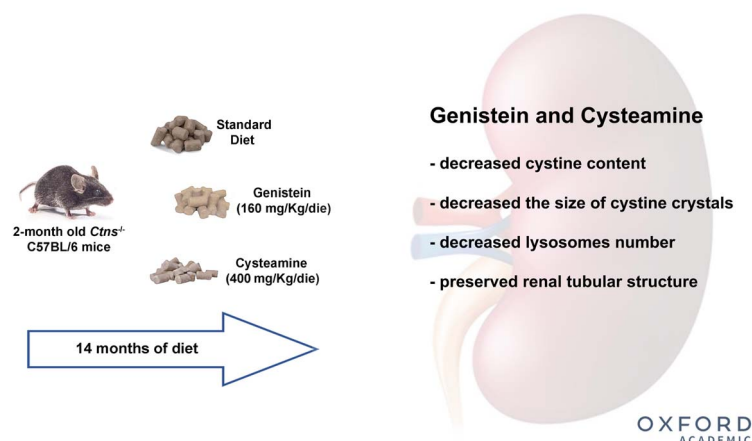*To whom correspondence should be addressed at: Renal Diseases Research Unit, Genetics and Rare Diseases Research Area, Bambino Gesù Children's Hospital, IRCCS, Viale di San Paolo 15, 00146 Rome, Italy. Tel: +39 0668592997; Email: l_rega@libero.it

Abstract

Cysteamine is currently the only therapy for nephropathic cystinosis. It significantly improves life expectancy and delays progression to end-stage kidney disease; however, it cannot prevent it. Unfortunately, compliance to therapy is often weak, particularly during adolescence. Therefore, finding better treatments is a priority in the field of cystinosis. Previously, we found that genistein, an isoflavone particularly enriched in soy, can revert part of the cystinotic cellular phenotype that is not sensitive to cysteamine *in vitro*. To test the effects of genistein *in vivo*, we fed 2-month-old wild-type and $Ctns^{-/-}$ female mice with either a control diet, a genistein-containing diet or a cysteamine-containing diet for 14 months. Genistein (160 mg/kg/day) did not affect the growth of the mice or hepatic functionality. Compared with untreated mice at 16 months, $Ctns^{-/-}$ mice fed with genistein had lower cystine concentrations in their kidneys, reduced formation of cystine crystals, a smaller number of LAMP1-positive structures and an overall better-preserved parenchymal architecture. Cysteamine (400 mg/kg/day) was efficient in reverting the lysosomal phenotype and in preventing the development of renal lesions. These preclinical data indicate that genistein ameliorates kidney injury resulting from cystinosis with no side effects. Genistein therapy represents a potential treatment to improve the outcome for patients with cystinosis.

Graphical Abstract

Introduction

Nephropathic cystinosis (Online Mendelian Inheritance in Man 219800) is caused by mutations in the *CTNS* gene, which encodes for cystinosin, an H^+/cystine symporter that regulates cystine efflux from lysosomes (1). A lack of functional cystinosin causes extensive and ubiquitous accumulation of lysosomal cystine and the formation of crystals in most tissues. Enhanced apoptosis (2), mitochondrial dysfunction (3,4), oxidative stress (5), inflammation (6), aberrant autophagy (7,8) and endo-lysosomal dysfunction (9,10) in cystinotic models have also been reported. From a clinical standpoint, by the age of 6 months patients develop generalized proximal tubular dysfunction (i.e. Fanconi syndrome). Glomerular dysfunction subsequently develops, and if left untreated, end-stage kidney disease occurs around the age of 10 years (11). Cystinosis is a systemic disease. Progressively, most organs are involved, including the eyes, endocrine organs, muscles, skeleton, male reproductive system, peripheral nerves and central nervous system (12,13).

Currently, the only approved treatment for nephropathic cystinosis is cysteamine, which facilitates the clearance of lysosomal cystine (14). Cysteamine delays the progression toward end-stage kidney disease and delays or prevents several extra-renal manifestations (15); however, it has no effect on Fanconi syndrome in the kidney. Moreover, compliance and adherence to cysteamine therapy are limited by side effects, in particular, a foul odor and gastrointestinal discomfort. Although rare, patients may also develop neutropenia or allergic reactions (16). For these reasons, the cystinosis community is in need of new therapeutic approaches (17). An initial strategy focused on developing cysteamine formulations with an improved pharmacokinetic profile (18). Drug repurposing has also been considered a promising approach to treat cystinosis (19). Hematopoietic stem cell transplantation has shown encouraging results in mice (20), and a clinical trial is currently ongoing after *in vitro* gene therapy (NCT03897361). Alternatively, or in addition to the previous approaches, the use of drug combinations may reduce the dose of cysteamine required to clear lysosomal cystine and may target pathways that are unresponsive to cysteamine (21,22). To this end, we recently identified genistein and luteolin as compounds that improve or revert various aspects of the cystinosis phenotype, several of which are not responsive to cysteamine (21,23). Genistein and luteolin belong to the flavonoid family, and many flavonoids exhibit significant renoprotective effects because of their anti-inflammatory, antioxidant and antihypertensive properties (24).

In addition, we previously showed that genistein stimulates lysosomal exocytosis and, therefore, promotes the clearance of lysosomal cystine and rescues the abnormal morphology of the lysosomal compartment in cystinotic cells (23). Based on these findings, we determined whether genistein can reduce renal cystine accumulation *in vivo* and delay progression of kidney failure in a mouse model of cystinosis.

Results

Treatment with genistein is safe in wild-type and *Ctns*⁻/⁻ mice

Wild-type and cystinotic (*Ctns*⁻/⁻) female mice were fed from 2 to 16 months of age with a standard diet or with the same diet containing 160 mg/kg/day of genistein. The genistein dose was selected based on available data in the literature for mice with the same genetic background (C57BL/6 strain) (25). Growth was monitored every 2 months. No significant differences in body weight or length were observed (Supplementary Material, Fig. S1). At the end of the study, the mice were sacrificed to collect serum and tissue samples. The liver, kidneys, uterus and ovaries were inspected and weighed. We observed no significant differences in organ weight among the experimental groups (Table 1). Histology revealed normal ovarian parenchyma with dense ovarian stroma containing follicles at varying maturation stages (from primordial to primary and secondary types) and, occasionally, the corpora lutea. No significant differences were observed between the experimental groups and no changes in pathological features were observed (data not shown). Serum levels of alanine aminotransferase (ALT), aspartate aminotransferase (AST) and gamma glutamyl transferase (GGT) were within the normal range for all groups (Table 2).

Genistein reduces the levels of cystine in *Ctns*⁻/⁻ mice kidneys

The accumulation of cystine is a hallmark of cystinosis. Therefore, we measured the levels of cystine in the kidneys from *Ctns*⁻/⁻ and wild-type mice untreated or treated with genistein for 14 months. Following genistein treatment, we observed a 32% (interquartile range [IQR] [44–83.5], P = 0.038, Fig. 1A) median reduction of cystine content in the kidneys of *Ctns*⁻/⁻ mice. Cystine levels in both liver and muscles from *Ctns*⁻/⁻ mice were comparable between untreated and genistein treated animals (data not shown). For comparison, we measured cystine concentration in the kidneys of *Ctns*⁻/⁻ mice treated with 400 mg/kg/day of cysteamine from age 2 to 16 months and observed a 93% (IQR [3–36], P < 0.001, Fig. 1A) median reduction in cystine content.

Large crystals were identified within the abnormal lysosome-like structures of the *Ctns*⁻/⁻ kidneys at the ultrastructural level (median size 0.72 [IQR 0.41–1.28], Fig. 1B, black arrow, red false color). Genistein caused a 70% reduction in lysosomal crystal size (median size 0.22 [IQR 0.10–0.36], P < 0.001, Fig. 1B, black arrow, green false color). We observed a similar reduction in crystal size in samples obtained from mice treated with cysteamine (median size 0.23 [0.13–0.37], P < 0.001, Fig. 1B), compared with untreated animals.

Genistein rescues the abnormalities of the lysosomal compartments in *Ctns*⁻/⁻ mouse kidneys

We previously demonstrated that genistein promotes the clearance of lysosomal cystine and rescues the abnormal lysosomal morphology by stimulating the activity of the transcription factor EB (TFEB) in cystinotic cells (23). Based on these previous *in vitro* results, we first assessed the effects of genistein on the endogenous expression of TFEB in total kidney tissue homogenates. Immunoblot analysis revealed a 2.6-fold reduction in the levels of endogenous TFEB in *Ctns*⁻/⁻ kidneys, compared with the wild-type organs (0.35 [IQR 0.15–0.49] versus 0.93 [IQR 0.69–1.23], P = 0.002, Fig. 2A). TFEB levels were upregulated by 1.8-fold in *Ctns*⁻/⁻ kidneys following genistein treatment (0.65 [IQR 0.49–0.87], P = 0.02, Fig. 2A). No changes in TFEB levels were observed in wild-type kidneys following treatment with genistein (0.46 [IQR 0.13–1.97], Fig. 2A). Following cysteamine treatment, TFEB levels were increased 3.4-fold in *Ctns*⁻/⁻ kidneys (1.21 [IQR 0.70–2.25], P = 0.008, Fig. 2A).

Next, we determined the effects of genistein on the lysosomal compartment in the kidneys (Fig. 2B). Immunofluorescence analysis of lysosomal-associated membrane protein 1 (LAMP1)

Table 1. Organ weights from 16-month-old female mice expressed as percent of body weight

	Wild-type control diet n = 9	Wild-type genistein n = 7	Ctns$^{-/-}$ control diet n = 7	Ctns$^{-/-}$ genistein n = 6
Kidneys	1.43 [1.42–1.74]	1.52 [1.44–1.78]	1.20 [1.17–1.45]	1.27 [0.8–1.34]
Uterus and ovaries	0.45 [0.23–0.73]	0.66 [0.42–0.74]	0.41 [0.29–0.70]	0.60 [0.57–0.89]
Liver	5.17 [4.51–6.63]	6.13 [4.82–7.11]	5.00 [4.40–5.42]	5.10 [4.66–5.17]

Note: Data are presented as median [IQR, 25th–75th percentile]. Differences among groups are not significant, nonparametric Kruskal–Wallis test.

Table 2. Parameters of liver function in 16-month-old female mice

	Wild-type control diet n = 9	Wild-type genistein n = 8	Ctns$^{-/-}$ control diet n = 8	Ctns$^{-/-}$ genistein n = 7	Normal range
ALT U/l	28 [21.3–56]	32.7 [19.6–62.7]	30.7 [17.8–52.9]	19 [14–32]	26–77
AST U/l	135.9 [88.8–210]	162 [84.7–219.1]	161.5 [133–186.5]	147 [40.5–215]	54–269
GGT U/l	8 [6–14]	8.5 [7.25–41]	6 [3.25–8.75]	8 [5–18]	0–50

Note: Data are presented as median [IQR, 25th–75th percentile]. Differences among groups are not significant, nonparametric Kruskal–Wallis test.
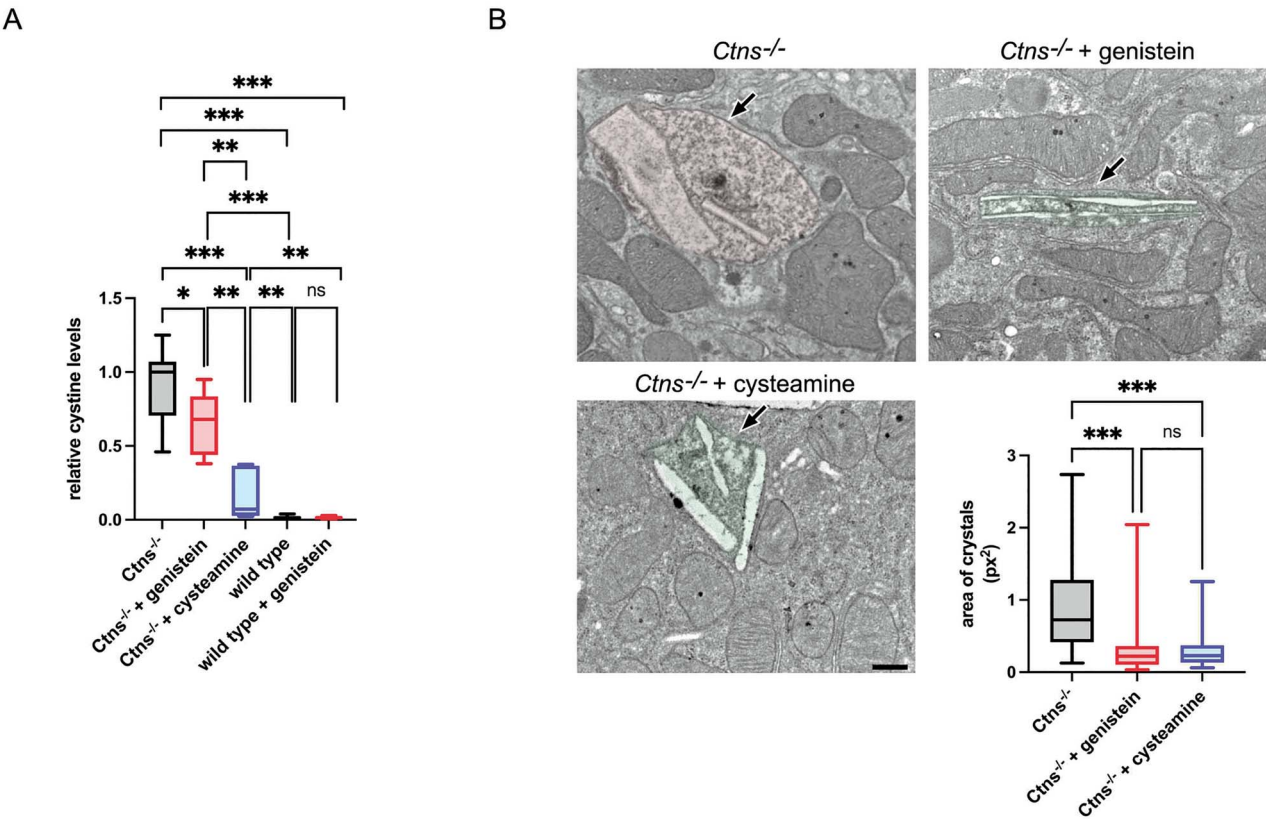

Figure 1. Genistein reduces the accumulation of cystine in the kidneys of Ctns$^{-/-}$ mice. (**A**) Cystine levels were measured in kidneys from Ctns$^{-/-}$ and wild-type mice that were untreated or treated with genistein (n = 9 mice for each experimental group). For comparison, Ctns$^{-/-}$ mice were also treated with cysteamine (n = 5 mice). The data are normalized to the protein concentration and expressed as relative levels compared with Ctns$^{-/-}$ untreated mice. (**B**) Representative kidney electron micrographs from Ctns$^{-/-}$ mice that were untreated or treated with genistein or cysteamine showing the presence of intracellular cystine crystals in lysosome-like structures (black arrows). The measured single crystal areas (px²) are shown in the bottom right panel. Scale bar: 400 nm. Each box plot represents the median and the 25th and 75th percentiles. Error bars represent the smallest and the largest values. Differences between groups were compared using the nonparametric Kruskal–Wallis test and, if significant, the unpaired Mann–Whitney U test was applied. *$P < 0.05$; **$P < 0.01$; ***$P < 0.001$. ns, not statistically significant.

in kidneys harvested from untreated Ctns$^{-/-}$ mice revealed an enlarged lysosomal compartment as assessed by the number (1553 [IQR 1107–2050] versus 69 [IQR 30–151], $P < 0.001$, Fig. 2C), the relative area (2.64 [IQR 1.14–3.58] versus 0.13 [IQR 0.04–0.24], $P < 0.001$, Fig. 2D) and the absolute area of LAMP1-positive structures (1190 [IQR 513–1609] versus 57 [IQR 18–106], $P < 0.001$, Fig. 2E) in Ctns$^{-/-}$ versus wild-type mice. Following genistein treatment, we observed a 40% reduction in the number of

LAMP1-positive structures (928 [IQR 695.5–1214], $P < 0.001$) and a 50% decrease in the relative and absolute area of LAMP1-positive structures in kidney sections from Ctns$^{-/-}$ mice (1.36 [IQR 0.88–2.23] and 609 [IQR 397–1002], respectively, $P < 0.001$, Fig. 2C–E). Following cysteamine treatment, we observed a 70% reduction in the number of LAMP1-positive structures (467 [IQR 267–711], $P < 0.001$), a 76% decrease in the relative area of LAMP1-positive structures (0.63 [IQR 0.29–0.94], $P < 0.001$) and a 72% decrease in
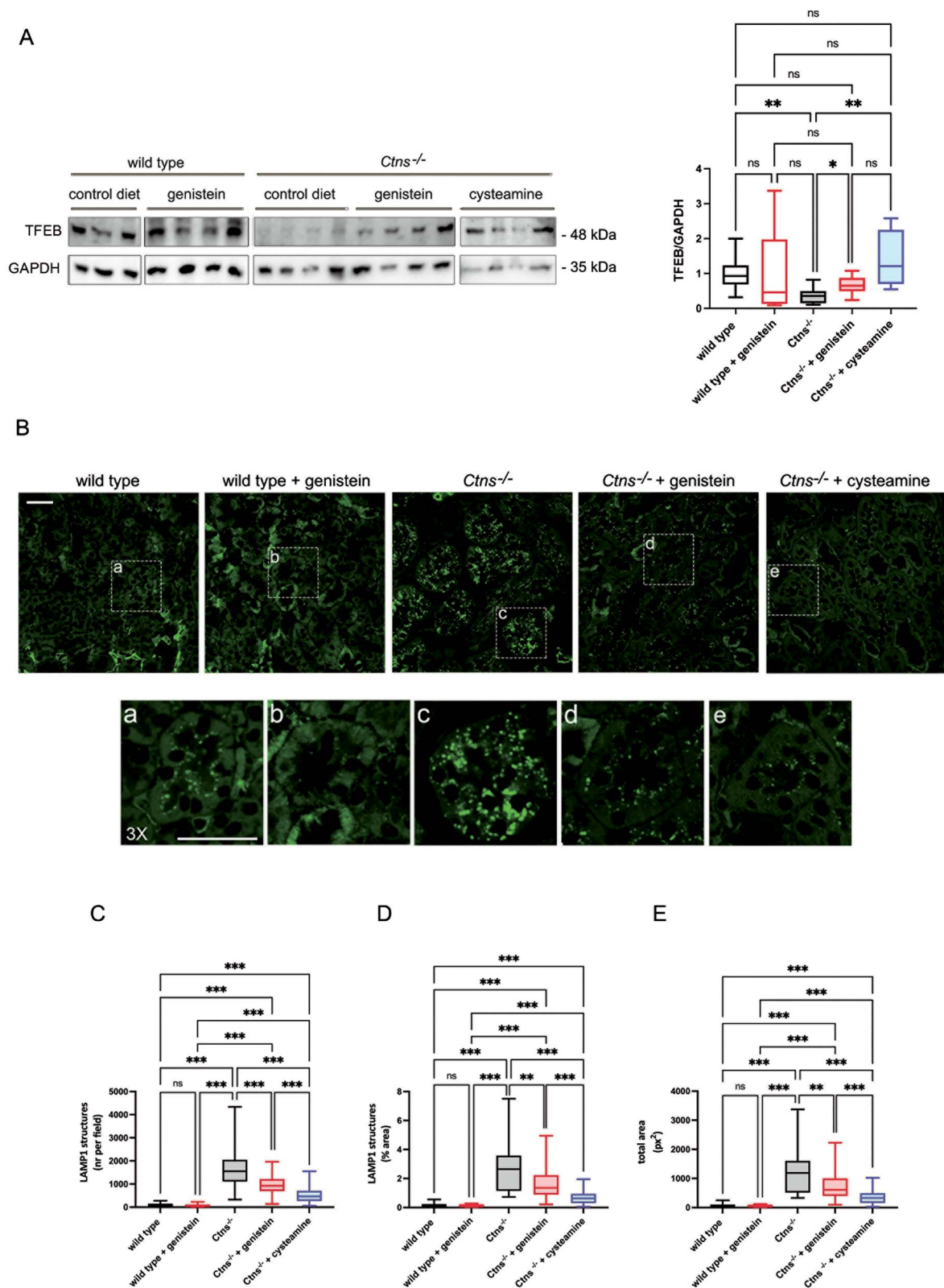
Figure 2. Genistein rescues TFEB levels and lysosomal abnormalities in the renal parenchyma of *Ctns*^{−/−} mice. (**A**) Western blot and densitometric analysis of TFEB and GAPDH levels in kidneys from wild-type ($n = 9$) and *Ctns*^{−/−} mice ($n = 8$) following treatment with genistein ($n = 9$ mice) or cysteamine ($n = 4$). In a representative western blot each lane corresponds to a single animal. The graph shows relative values of TFEB levels normalized against GAPDH. (**B**) Representative fluorescence images of LAMP1 staining in kidney sections from wild-type and *Ctns*^{−/−} mice after treatment with genistein or cysteamine ($n = 5$ mice) (scale bar: 10 μm). Three-fold magnification insets are shown on the bottom (a–e) (scale bar: 30 μm). Images were quantified for (**C**) the number of LAMP1 structures and the (**D**) percentage or (**E**) total area (px^2) of LAMP1-positive structures. Each box plot represents the median and the 25th and 75th percentiles. Error bars represent the smallest and the largest values. Differences between groups were compared using the nonparametric Kruskal–Wallis test and, if significant, the unpaired Mann–Whitney U test was applied. *$P < 0.05$; **$P < 0.01$; ***$P < 0.001$. ns, not statistically significant.
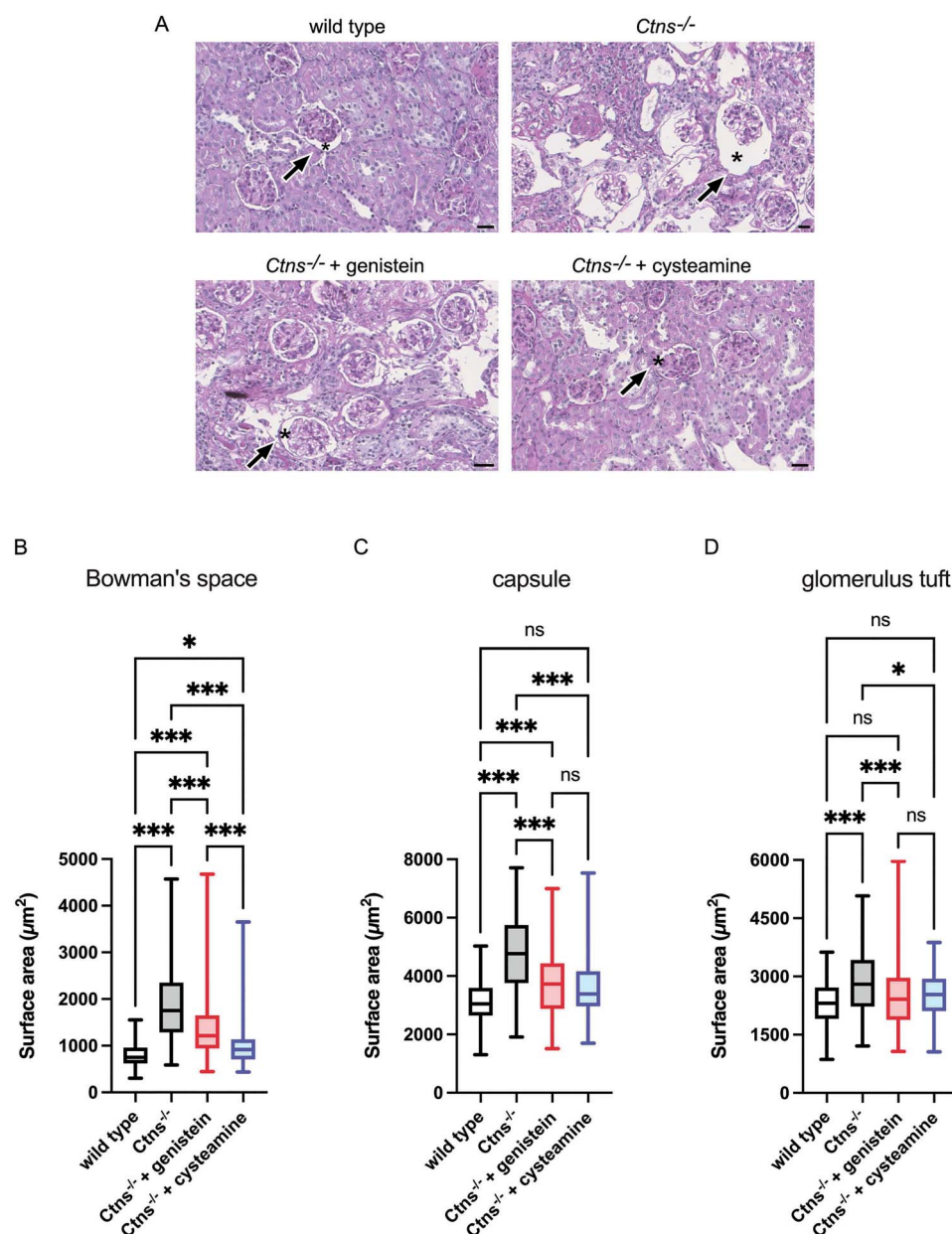
Figure 3. Genistein prevents dilatation of the Bowman's capsule in *Ctns*$^{-/-}$ mice. (**A**) Representative images (Periodic acid–Schiff stain) of kidneys harvested from wild-type and *Ctns*$^{-/-}$ mice that were untreated or treated with genistein or cysteamine. Arrows and asterisks indicate the Bowman's space. Scale bar: 25 μm. The surface area (μm^2) of the (**B**) Bowman's space, (**C**) Bowman's capsule and (**D**) glomerular tuft was quantified in individual glomeruli; each box plot represents the median and the 25th and 75th percentiles. Error bars represent the smallest and the largest values. Differences between groups were compared using the nonparametric Kruskal–Wallis test and, if significant, the unpaired Mann–Whitney U test was applied. *$P < 0.05$; **$P < 0.01$; ***$P < 0.001$. ns, not statistically significant.

the absolute area of LAMP1-positive structures (330 [IQR 154–493], $P < 0.001$) (Fig. 2C–E). No changes were observed in the wild-type animals.

These results indicate that *in vivo* genistein treatment improves the known abnormalities of the lysosomal compartment that are observed in cystinosis. This effect may be mediated, at least in part, by the upregulation of TFEB protein levels in *Ctns*$^{-/-}$ kidneys.

Genistein prevents morphological changes in the renal parenchyma and delays kidney function deterioration

Cystinosis kidneys develop progressive changes characterized by the dilation of tubules and the Bowman's space. This is associated

with the formation of atubular glomeruli (26). Accordingly, we observed a significant enlargement of Bowman's space in *Ctns*$^{-/-}$ mice (1762 μm [IQR 1305–2439] versus 749.9 μm [IQR 621.6–960.8], $P < 0.001$, Fig. 3A and B, black arrows and asterisks). The total area of the Bowman's capsule and of the glomerular tuft was also increased in *Ctns*$^{-/-}$ mice compared with the wild-type mice (3800 [IQR 1914–4854] versus 2644 [IQR 1303–3048] and 2798 [IQR 2223–3425] versus 2312 [IQR 1911–2717], respectively, $P < 0.001$, Fig. 3C and D). Following genistein treatment, the enlargement of Bowman's space (1222 [IQR 945–1654], $P < 0.001$, Fig. 3A and B) and capsule (3764 [IQR 2937–4540], $P < 0.001$, Fig. 3A and C) was significantly reduced, compared with the untreated *Ctns*$^{-/-}$ mice. The same effect on Bowman's space and capsule areas was
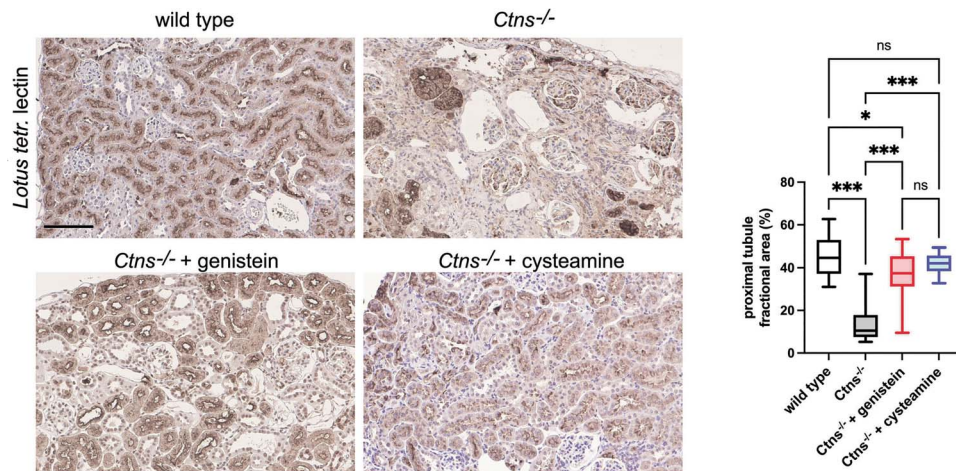
Figure 4. Genistein preserves renal proximal tubules in *Ctns*−/− mice. Representative images of LT-lectin-stained kidney cortex sections obtained from kidneys harvested from wild-type and *Ctns*−/− mice that were untreated, or treated with genistein or cysteamine. Scale bar: 100 μm. The fractional area of the proximal tubules was measured in microscopic fields. Each box plot represents the median and the 25th and 75th percentiles. Error bars represent the smallest and the largest values. Differences between groups were compared using the nonparametric Kruskal–Wallis test and, if significant, the unpaired Mann–Whitney *U* test was applied. *$P < 0.05$; **$P < 0.01$; ***$P < 0.001$. ns, not statistically significant.

observed after treatment with cysteamine (917.3 [IQR 708.3–1134], $P < 0.001$, Fig. 3A and B; 3388 [IQR 2969–4161], $P < 0.001$, Fig. 3A and C).

The proximal tubular fraction of the cortical parenchyma was assessed by testing the affinity for *Lotus tetragonolobus* (LT) lectin. As expected, we observed that the area occupied by the proximal tubules was reduced in *Ctns*−/− kidneys compared with wild-type kidneys (10.5% [IQR 7.5–17.8] versus 44.6% [IQR 37.2–52.9], $P < 0.001$, Fig. 4). Following treatment with genistein, the area occupied by LT-lectin positive structures was significantly increased in *Ctns*−/− mice (37.4% [IQR 31.2–45.4], $P < 0.001$, Fig. 4). Similar results were observed after treatment with cysteamine (42.1% [IQR 38.4–45.7], $P < 0.001$).

Finally, we assessed the effects of genistein and cysteamine treatment on kidney function. Creatinine clearance was reduced by 56% in untreated *Ctns*−/− mice compared with the wild-type animals (0.44 [IQR 0.34–0.56] versus 1 [IQR 0.75–1.21], $P < 0.001$, Fig. 5). Creatinine clearance was restored following treatment with genistein (0.62 [IQR 0.55–1.21], $P < 0.05$, Fig. 5) or cysteamine (0.76 [IQR 0.69–0.85], $P < 0.05$, Fig. 5). We also monitored urinary levels of low molecular weight proteins (CC16), glucose, albumin, urine volume (Fig. 6 and Supplementary Material, Table S1) and phosphate (Supplementary Material, Table S1), every 2 months. We observed increased low molecular weight proteinuria, glucosuria, albuminuria and polyuria in *Ctns*−/− mice, compared with the wild-type animals; however, we did not observe statistically significant differences following genistein treatment (Fig. 6). Conversely, a significant protection of renal function parameters was observed after cysteamine treatment (Fig. 6).

Discussion

We previously observed a significant improvement in the cystinotic phenotype *in vitro* after incubating cells with genistein (23). In the present study, we determined whether these changes could also be observed *in vivo*. We used the *Ctns* knockout mouse model with a C57BL/6 background that was generated by Nevo *et al.* (27). The renal Fanconi syndrome was significantly milder, compared with that of previous reports (28); however, the causes of this discrepancy are currently under investigation in our
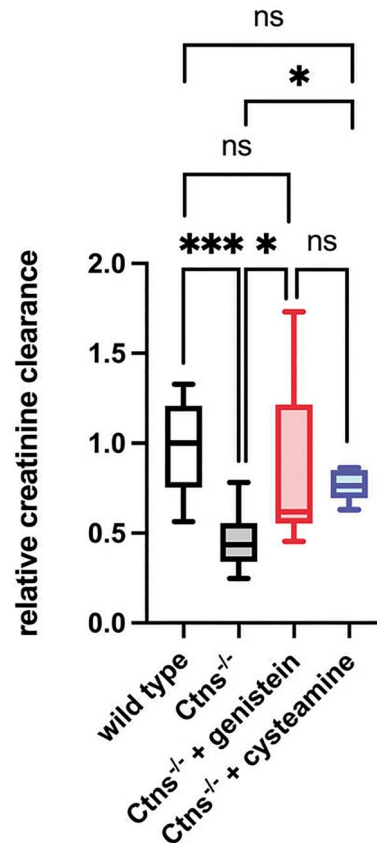
Figure 5. Genistein improves creatinine clearance in 16-month-old *Ctns*−/− mice. Creatinine clearance is shown for untreated and treated mice relative to the wild-type animals. Each box plot represents the median and the 25th and 75th percentiles. Error bars represent the smallest and the largest values. Differences between groups were compared using the nonparametric Kruskal–Wallis test and, if significant, the unpaired Mann–Whitney *U* test was applied. *$P < 0.05$; **$P < 0.01$; ***$P < 0.001$. ns, not statistically significant.

laboratory. This cystinotic mouse model has been widely used to obtain key insights in the pathophysiology of cystinosis (9,26, 29–32) and to develop new therapeutic strategies (30,33–35).

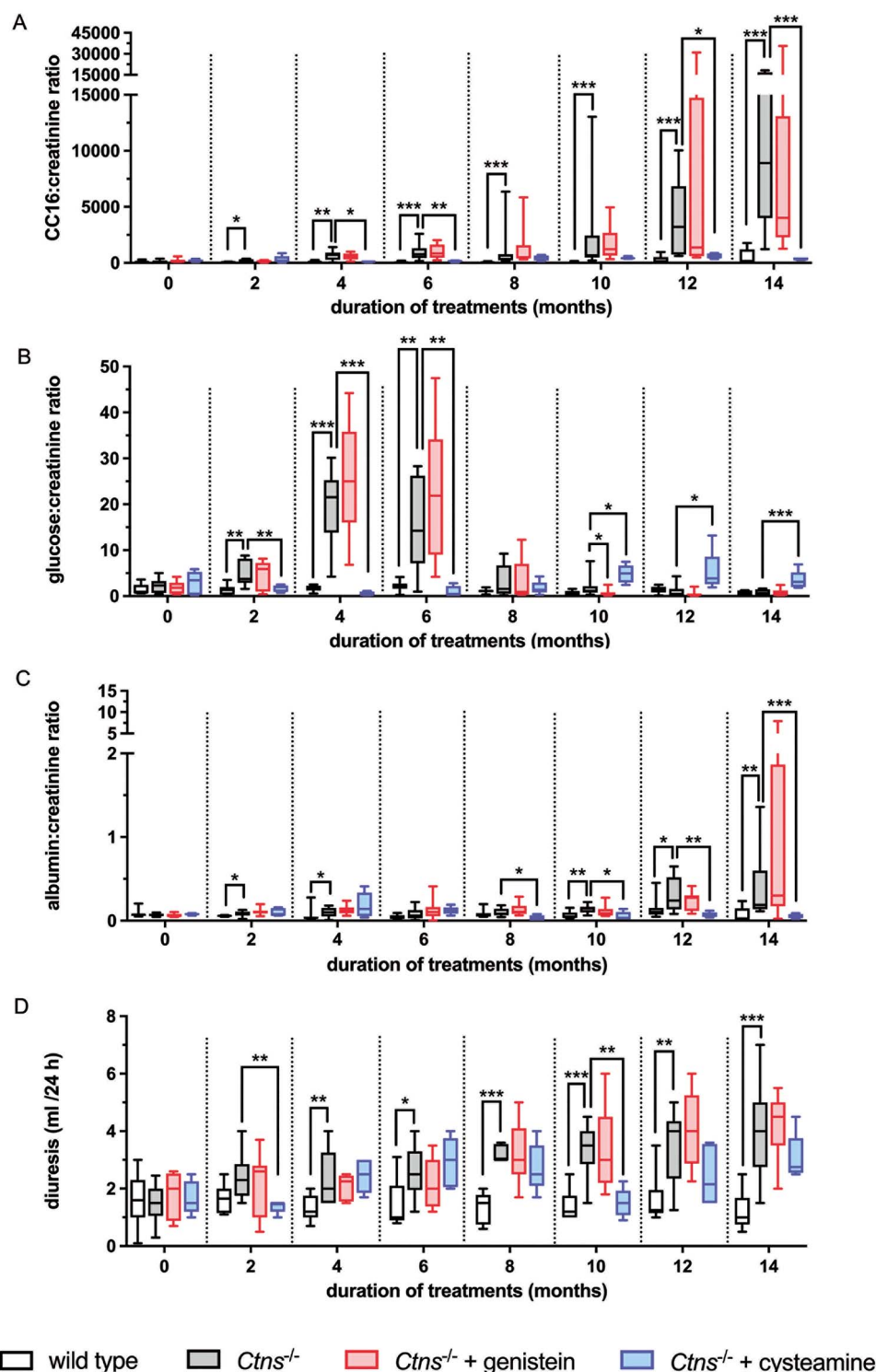**Figure 6.** Parameters of kidney function. Levels of urinary (**A**) low molecular weight proteins (CC16), (**B**) glucose and (**C**) albumin and (**D**) 24-h urine volume were checked every 2 months in wild-type and *Ctns*$^{-/-}$ mice that were untreated or treated with genistein or cysteamine. Values for CC16, glucose and albumin were normalized to creatinine (mg/ml). Each box plot represents the median and the 25th and 75th percentiles. Error bars represent the smallest and the largest values. Differences between groups were compared using the nonparametric Kruskal–Wallis test and, if significant, the unpaired Mann–Whitney *U* test was applied. *$P < 0.05$; **$P < 0.01$; ***$P < 0.001$. (Statistically significant differences are presented for wild-type versus *Ctns*$^{-/-}$ mice and genistein- or cysteamine-treated *Ctns*$^{-/-}$ mice versus untreated *Ctns*$^{-/-}$ mice. Further statistical comparisons are shown in Supplementary Table S1.)

Our study revealed that treatment with genistein ameliorates renal injury in cystinotic mice. Genistein belongs to the flavonoid family. These compounds, derived from plants, have already been evaluated for their renoprotective activity under various conditions (24). These include models of kidney injury induced by cisplatin (36) or gentamicin (37), fructose-induced hypertension (38), unilateral ureteral occlusion (39) and nephrotic syndrome (40). The protective effects of flavonoids in these models

have been ascribed to their anti-inflammatory, anti-oxidative, antiapoptotic and pleiotropic activities. Using an unbiased cell-based approach, we recently identified another flavonoid, luteolin, and demonstrated its beneficial effects on the cystinotic phenotype *in vitro* and in zebrafish (21). This further supports the potential role of this class of compounds for the treatment of nephropathic cystinosis and *in vivo* studies of luteolin in rodent models of cystinosis are underway.

The choice of genistein in the present study is based on our previous results showing that treatment of proximal tubular cells obtained from cystinotic patients reduces cystine levels and lysosomal engulfment through the activation of TFEB (23). In the same work, we also observed the downregulation of TFEB in cells lacking cystinosin (23). Similarly, Zhang *et al.* (41) have also demonstrated that endogenous TFEB is downregulated in *Ctns*$^{-/-}$ mouse fibroblasts. Our results in cystinotic mice confirm the *in vitro* data. Namely, we observed that renal cystine accumulation and the size of lysosomes in renal cells are reduced following treatment with genistein (Figs 1A and 2B–E). We also confirmed that TFEB protein levels are downregulated in kidney extracts obtained from *Ctns*$^{-/-}$ mice and are restored to wild-type levels after genistein treatment (Fig. 2A). We also observed a concomitant reduction in the size of cystine crystals in the renal parenchyma. These results are similar to that reported recently by Nakamura *et al.* (42) for oxalate nephropathy. They showed that TFEB activation plays a critical role in preventing the development of chronic renal lesions secondary to calcium oxalate crystal-induced lysosomal damage (42). TFEB knockout in the proximal tubules significantly accelerated the development of oxalate-induced kidney injury, highlighting the physiological relevance of TFEB activation in response to lysosomal damage.

The expression and activity of TFEB are known to be upregulated by genistein (43). Therefore, genistein is an attractive therapeutic option in lysosomal storage diseases and other pathological conditions that are ameliorated by TFEB activation. In addition to TFEB, genistein has other molecular targets, including the epidermal growth factor receptor, phosphoinositide 3-kinase/Akt, mitogen-activated protein kinase and nuclear factor-kB (44). Therefore, we cannot exclude that the effects we observed in nephropathic cystinosis mice may also be secondary to the modulation of these other pathways. TFEB protein levels were not altered in wild-type mice following treatment with genistein; however, these results do not exclude the possibility that TFEB may have been activated by genistein in wild-type animals. Contrary to previous *in vitro* observations (23,41), in which TFEB expression was unaffected by cysteamine treatment, our study surprisingly showed a restoration of TFEB levels in the kidneys of *Ctns*$^{-/-}$ mice treated with cysteamine. This may be secondary to the cysteamine-mediated protective effect on kidney injury in our experimental setting. Further studies are needed to demonstrate a direct effect of cysteamine on TFEB activation.

Although clearly beneficial, genistein did not completely prevent kidney injury in *Ctns*$^{-/-}$ mice (Figs 3–6 and Supplementary Material, Table S1). In particular, we did not observe a clear benefit of genistein on Fanconi syndrome parameters, despite significant protection against the development of parenchymal lesions and kidney failure. This may have been in part secondary to the modest effect of genistein on renal cystine accumulation (~30%, Fig. 1A) and/or to the size of the cohort. In fact, a more detailed analysis of the results obtained in the *Ctns*$^{-/-}$ genistein-treated group indicates that the data were not homogeneous, with two animals developing high low-molecular weight proteinuria, whereas the remaining seven mice had lower levels compared

with the untreated group. The 400 mg/kg/day dose of cysteamine was selected based on data from Cherqui *et al.* (45), in which a 50% reduction of cystine content was observed in the kidneys of mice treated for 60 days. Unlike what happens in humans, cysteamine was very efficient at preventing the development of renal lesions in mice (Fig. 3), which did not enable an assessment of the benefits of a combined therapy with cysteamine and genistein. Several elements may explain the differences in the response to cysteamine between mice and humans. First, mice do not develop very early onset Fanconi syndrome; thus, the mouse model may not fully recapitulate the human condition. Second, mice were treated very early before developing significant Fanconi syndrome. In contrast, humans are usually treated after being diagnosed with severe proximal tubulopathy. Finally, the cysteamine dose used in the present may be higher than the dose suggested in humans (1.30–1.95 g/m^2/day) corresponding approximately to 30–50 mg/kg/day (46). Therefore, additional studies are needed to identify a lower dose of cysteamine that is less effective, to determine whether the two drugs have an addictive effect.

Combined therapy with cysteamine and genistein could potentially reduce the dose of cysteamine needed to achieve cystine clearance, which would be extremely beneficial for mitigating the side effects that are associated with limited patient compliance (47). This association is also attractive because it would combine drugs that act through different mechanisms and potentially yielding synergistic effects. While cysteamine allows the clearance of cystine through the formation of mixed disulfides, genistein clears cell cystine content by TFEB-induced lysosomal exocytosis (23) and stimulates new lysosome synthesis.

Another potential beneficial effect of genistein in cystinosis may be associated with its effects on bones. In our previous study, we demonstrated that bone alterations (reduced bone mineral density and bone volume) and decreased mineralization that occur in cystinosis are also the result of primary defects in bone cells (48). Genistein has also been shown to have a protective effect against osteoporosis (49). It improves abnormal bone metabolism in diabetic rats, presumably through its hypoglycemic and anti-inflammatory effects (50). We found no significant difference in trabecular and cortical parameters between the groups of 16-month-old wild-type and *Ctns*$^{-/-}$ mice (data not shown). We cannot exclude that these results were affected by the aging and the related bone loss of our C57BL/6 background animal model that may prevent our assessment of the effect of genistein on the skeleton.

Genistein is particularly rich in soy. Patients with nephropathic cystinosis may be advised to increase their consumption of soy and soy-based products; however, the intake of genistein in the present study (160 mg/kg/day) was much higher than what would be expected from a soy-rich diet. Therefore, such an indication is questionable and should be confirmed in future studies. Of note, genistein is primarily eliminated by the kidneys (51). Chronic kidney disease may therefore cause genistein accumulation. In our experimental model, however, creatinine clearance was similar to that of wild-type animals (Fig. 5).

Genistein is a phytoestrogen, but we did not observe any abnormal effects on the genital organs after animal sacrifice. We could not test the hormonal profile during the study because blood sampling was insufficient and only female animals, which are known to accumulate more cystine (34), were examined. Although genistein is commercially available and used in human subjects, it should probably be addressed in regard to cystinosis. It should also be noted that male patients with nephropathic cystinosis frequently exhibit hypogonadotropic

hypogonadism and that azoospermia almost always occurs in adult patients (52).

In conclusion, genistein mitigated kidney disease in a mouse model of nephropathic cystinosis. Because of safety profile of genistein in humans, these results indicate that this molecule represents a potential candidate for treating this disease. Additional preclinical studies are needed to determine the potential synergistic effects of genistein with cysteamine and to exclude negative effects on the male and female reproductive systems.

Materials and Methods
Mouse maintenance and drug administration

Ctns knockout mice (C57BL/6 background) were kindly provided by Dr Corinne Antignac (27). Animal care and experimental procedures were conducted in accordance with the European 2010/63/EU directive on the protection of animals used for scientific purposes and authorized by the Italian Ministry of Health (authorization number 66/2018-PR).

Two-month-old female wild-type and *Ctns*$^{-/-}$ ($n = 9$ per group) mice were fed with a control diet (4RF21 diet, Mucedola Srl, Settimo Milanese, Italy) or with the same diet containing 1.17 g of genistein per kg (ACEF Spa, Fiorenzuola D'Arda, Italy). An additional group of 2-month-old female *Ctns*$^{-/-}$ mice ($n = 5$) was fed with 2.93 g of cysteamine bitartrate per kg. Cysteamine powder was obtained from Cystagon® capsules (Recordati Rare Diseases, Milan, Italy) used for human therapy. The estimated corresponding doses were 160 mg/kg/day for genistein and 400 mg/kg/day for cysteamine. These calculations were made based on preliminary data showing that mice with an average weight of 22 g eat on average 3 g of food per day.

Mice were acclimatized in metabolic cages for 24 h, and urine was collected in the following 24 h in the presence of 0.1% sodium azide and 1X protease inhibitors (Thermo Scientific). Mouse weight and length were recorded before entering the metabolic cages. Blood was collected at the sacrifice to obtain serum. Urine and serum analyses were performed by the veterinary laboratory Appialab Srl (Rome, Italy). Creatinine clearance was calculated by the formula: creatinine clearance (ml/min) = urine creatinine (mg/dl) × 24 h urine volume (ml)/serum creatinine (mg/dl) × 1440 min. Creatinine clearance was normalized against mouse body weight.

Western blotting

Proteins were extracted by sonicating the tissues in RIPA buffer, containing protease and phosphatase inhibitors (Thermo Scientific) and centrifuged for 10 min at 13 000 rpm at 4°C.

Protein concentrations were measured using the Bio-Rad Protein Assay (Bio-Rad Laboratories, Inc., Hercules, CA) according to the manufacturer's instructions. Proteins were separated under reducing condition by electrophoresis on 8% gels (NuSep, Köln, Germany) and immunoblotted onto polyvinylidene difluoride membranes. The membranes were blocked with 5% BSA diluted in Tris-buffered saline, 0.1% Tween 20 and incubated overnight with rabbit anti-TFEB (1:1000) (#A303-673A Bethyl laboratories Inc., Montgomery, Texas) or rabbit anti-GAPDH (1:1000) (#5174 Cell Signalling, Danvers, Massachusetts). Following the incubation with horseradish peroxidase (HRP), secondary antibody conjugates IgG (Jackson ImmunoResearch Europe Ltd, Cambridge House, UK). Immunoblots were developed with LiteAblot EXTEND (EuroClone, Milan, Italy) and acquired with the ChemiDoc XRS System (Bio-Rad). Density of the bands was quantified by Image Lab software (Bio-Rad).

Electron microscopy

Small pieces of kidney tissue were fixed with 1% glutaraldehyde prepared in 0.2 M HEPES buffer (pH 7.3) for 30 min (RT). Then samples were post-fixed in OsO4 and uranyl acetate, dehydrated, embedded in Epon and polymerized at 60°C for 72 h. For each sample, 60 nm thick sections were cut using a Leica EM UC7 ultramicrotome (Leica Microsystems, Vienna, Austria). Electron microscopy images were acquired from these sections using a FEI Tecnai-12 electron microscope (FEI, Eindhoven, the Netherlands) equipped with a VELETTA CCD digital camera (Soft Imaging Systems GmbH, Munster, Germany). The area of crystals (px^2) was quantified within 16X fields of view (>45 crystals for each experimental condition).

Histology, immunofluorescence and morphometry

Sections were stained with Periodic Acid Schiff Kit (P.A.S.) (#04-130802, Bio-Optica, Milano, Italy) according to the manufacturer's instructions.

Immunohistochemistry was performed on 3 μm thick sections obtained from formalin-fixed tissue embedded in paraffin. After dewaxing and rehydrating, heat-induced epitope retrieval was performed by boiling the slides with EDTA (pH 9) (Dako, Glostrup, Denmark). Tissue slides were blocked in 5% BSA for 1 h. Sections were incubated overnight at 4°C with mouse monoclonal LAMP1 (1:100) (#sc-20011, Santa Cruz Biotechnology, Inc., Santa Cruz, CA) or biotinylated LT-lectin (1:100) (#B-1325-2, Vector Laboratories). The primary antibody LAMP1 was revealed with the secondary antibody Alexa Fluor goat anti-mouse 488 (Applied Biosystems, Life Technologies, Carlsbad, CA, USA). For nuclear staining, 49,6-diamidino-2-phenylindole was added for 5 min before section mounting with glycerol/PBS (1:1).

To quantify lysosomal morphology, we assessed the number, the percentage and total area of LAMP1-positive structures within >50 random 60X fields of view for each experimental condition by Image J software.

LT-lectin was revealed with streptavidin-HRP kit (ready to use) (#K3954, Dako, Carpinteria, USA) and the peroxidase DAB kit (Dako, Carpinteria, USA). Counterstaining was performed with hematoxylin solution Gill2.

Morphometric determinations of proximal tubule fractional area were made in sections stained with LT-lectin as previously described (53). Briefly, five fields of the subcapsular cortex for each mouse were analyzed using microscopic fields at ×20 magnification. The fractional area of proximal tubule was measured within >40 random fields for each experimental condition after digital contrasting using the QuPath software (54).

The areas of both glomerular capsule and tuft were measured on P.A.S.-stained sections by NDP.view2 Image viewing software. The area of the Bowman's space was determined by subtracting the glomerular tuft area from the total area within the capsule in >80 glomeruli.

LC–MS determination of cystine

Dissected tissues were homogenized in 10 mM N-ethylmaleimide. Protein fraction was obtained following precipitation in 10% 5-sulfosalicylic acid and centrifugation at 20 000×*g* for 20 min at 4°C. Protein pellet was resuspended in 100 mM NaOH and assayed by the Bio-Rad Protein Assay according to the manufacturer's instructions. Supernatant (50 μl) was mixed with 50 μl of the internal standard solution (Cystine d6) and vortexed for 5 s; then the mixture was extracted with 200 μl of acetonitrile, vortexed at

least 30 s and then centrifuged at 13 000 rpm for 9 min. Liquid chromatography and mass spectrometry analysis was performed by a UHPLC Agilent 1290 Infinity II 6470 (Agilent Technologies) equipped with an ESI-JET-STREAM source operating in the positive ion (ESI+) mode. MassHunter Workstation (Agilent Technologies) software was used to control the equipment and analyze the data. The separation column was InfinityLab Poroshell 120 HILIC 1.9 μm 100 × 2.1 mm (Agilent Technologies). Validation of the method was performed based on the US Food and Drug Administration (FDA) guideline for industry bioanalytical method validation (FDA 2013) and European Medicines Agency (EMA) guideline (EMA 2011). The validation of the assay was performed including selectivity, specificity, linearity and limit of quantification, accuracy and precision, matrix effects and recovery, and stability.

Statistics

Data are presented as median and IQR [25th–75th] unless otherwise specified in the figure legends. Differences among groups were compared by the nonparametric Kruskal–Wallis test. If differences were significant, pairwise comparisons were evaluated by the Mann–Whitney U test. P-values <0.05 were considered significant. GraphPad Prism software version 9 was used for all statistical analyses.

Supplementary Material

Supplementary Material is available at *HMG* online.

Acknowledgements

Funding

References

1. Kalatzis, V., Cherqui, S., Antignac, C. and Gasnier, B. (2001) Cystinosin, the protein defective in cystinosis, is a H+-driven lysosomal cystine transporter. *EMBO J.*, **20**, 5940–5949.
2. Taranta, A., Bellomo, F., Petrini, S., Polishchuk, E., De Leo, E., Rega, L.R., Pastore, A., Polishchuk, R., De Matteis, M.A. and Emma, F. (2017) Cystinosin-LKG rescues cystine accumulation and decreases apoptosis rate in cystinotic proximal tubular epithelial cells. *Pediatr. Res.*, **81**, 113–119.
3. Bellomo, F., Signorile, A., Tamma, G., Ranieri, M., Emma, F. and De Rasmo, D. (2018) Impact of atypical mitochondrial cyclic-AMP level in nephropathic cystinosis. *Cell. Mol. Life Sci.*, **75**, 3411–3422.
4. De Rasmo, D., Signorile, A., De Leo, E., Polishchuk, E.V., Ferretta, A., Raso, R., Russo, S., Polishchuk, R., Emma, F. and Bellomo, F. (2020) Mitochondrial dynamics of proximal tubular epithelial cells in nephropathic cystinosis. *Int. J. Mol. Sci.*, **21**, 192.
5. Sumayao, R., McEvoy, B., Newsholme, P. and McMorrow, T. (2016) Lysosomal cystine accumulation promotes mitochondrial depolarization and induction of redox-sensitive genes in human kidney proximal tubular cells. *J. Physiol.*, **594**, 3353–3370.
6. Prencipe, G., Caiello, I., Cherqui, S., Whisenant, T., Petrini, S., Emma, F. and De Benedetti, F. (2014) Inflammasome activation by cystine crystals: implications for the pathogenesis of cystinosis. *J. Am. Soc. Nephrol.*, **25**, 1163–1169.
7. Festa, B.P., Chen, Z., Berquez, M., Debaix, H., Tokonami, N., Prange, J.A., van de Hoek, G., Alessio, C., Raimondi, A., Nevo, N. *et al.* (2018) Impaired autophagy bridges lysosomal storage disease and epithelial dysfunction in the kidney. *Nat. Commun.*, **9**, 161.
8. Napolitano, G., Johnson, J.L., He, J., Rocca, C.J., Monfregola, J., Pestonjamasp, K., Cherqui, S. and Catz, S.D. (2015) Impairment of chaperone-mediated autophagy leads to selective lysosomal degradation defects in the lysosomal storage disease cystinosis. *EMBO Mol. Med.*, **7**, 158–174.
9. Raggi, C., Luciani, A., Nevo, N., Antignac, C., Terryn, S. and Devuyst, O. (2014) Dedifferentiation and aberrations of the endolysosomal compartment characterize the early stage of nephropathic cystinosis. *Hum. Mol. Genet.*, **23**, 2266–2278.
10. Ivanova, E.A., De Leo, M.G., Van Den Heuvel, L., Pastore, A., Dijkman, H., De Matteis, M.A. and Levtchenko, E.N. (2015) Endolysosomal dysfunction in human proximal tubular epithelial cells deficient for lysosomal cystine transporter cystinosin. *PLoS One*, **10**, e0120998.
11. Emma, F., Nesterova, G., Langman, C., Labbe, A., Cherqui, S., Goodyer, P., Janssen, M.C., Greco, M., Topaloglu, R., Elenberg, E. *et al.* (2014) Nephropathic cystinosis: an international consensus document. *Nephrol. Dial. Transplant.*, **29**, iv87–iv94.
12. Kasimer, R.N. and Langman, C.B. (2021) Adult complications of nephropathic cystinosis: a systematic review. *Pediatr. Nephrol.*, **36**, 223–236.
13. Topaloglu, R. (2021) Nephropathic cystinosis: an update on genetic conditioning. *Pediatr. Nephrol.*, **36**, 1347–1352.
14. Gahl, W.A., Reed, G.F., Thoene, J.G., Schulman, J.D., Rizzo, W.B., Jonas, A.J., Denman, D.W., Schlesselman, J.J., Corden, B.J. and Schneider, J.A. (1987) Cysteamine therapy for children with nephropathic cystinosis. *N. Engl. J. Med.*, **316**, 971–977.
15. Emma, F., vant. Hoff, W., Hohenfellner, K., Topaloglu, R., Greco, M., Ariceta, G., Bettini, C., Bockenhauer, D., Veys, K., Pape, L. *et al.* (2021) An international cohort study spanning five decades assessed outcomes of nephropathic cystinosis. *Kidney Int.*, **100**, 1112–1123.
16. Gahl, W.A., Thoene, J.G. and Schneider, J.A. (2002) Medical progress: cystinosis. *N. Engl. J. Med.*, **347**, 111–121.
17. Jamalpoor, A., Othman, A., Levtchenko, E.N., Masereeuw, R. and Janssen, M.J. (2021) Molecular mechanisms and treatment options of nephropathic cystinosis. *Trends Mol. Med.*, **27**, 673–686.
18. Berends, C.L., Pagan, L., van Esdonk, M.J., Klarenbeek, N.B., Bergmann, K.R., Moerland, M., van der Wel, V., de Visser, S.J., Büller, H., de Loos, F. *et al.* (2021) A novel sustained-release cysteamine bitartrate formulation for the treatment of cystinosis: pharmacokinetics and safety in healthy male volunteers. *Pharmacol. Res. Perspect.*, **9**, e00739.
19. Bellomo, F., De Leo, E., Taranta, A., Giaquinto, L., Di Giovamberardino, G., Montefusco, S., Rega, L.R., Pastore, A., Medina, D.L., Di Bernardo, D. *et al.* (2021) Drug repurposing in rare diseases: an integrative study of drug screening and transcriptomic analysis in nephropathic cystinosis. *Int. J. Mol. Sci.*, **22**, 12829.
20. Rocca, C.J. and Cherqui, S. (2019) Potential use of stem cells as a therapy for cystinosis. *Pediatr. Nephrol.*, **34**, 965–973.

21. De Leo, E., Elmonem, M.A., Berlingerio, S.P., Berquez, M., Festa, B.P., Raso, R., Bellomo, F., Starborg, T., Janssen, M.J., Abbaszadeh, Z. *et al.* (2020) Cell-based phenotypic drug screening identifies luteolin as candidate therapeutic for nephropathic cystinosis. *J. Am. Soc. Nephrol.*, **31**, 1522–1537.

22. Jamalpoor, A., Gelder, C.A., Yousef Yengej, F.A., Zaal, E.A., Berlingerio, S.P., Veys, K.R., Pou Casellas, C., Voskuil, K., Essa, K., Ammerlaan, C.M. *et al.* (2021) Cysteamine–bicalutamide combination therapy corrects proximal tubule phenotype in cystinosis. *EMBO Mol. Med.*, **13**, e13067.

23. Rega, L.R., Polishchuk, E., Montefusco, S., Napolitano, G., Tozzi, G., Zhang, J., Bellomo, F., Taranta, A., Pastore, A., Polishchuk, R. *et al.* (2016) Activation of the transcription factor EB rescues lysosomal abnormalities in cystinotic kidney cells. *Kidney Int.*, **89**, 862–873.

24. Vargas, F., Romecín, P., García-Guillén, A.I., Wangesteen, R., Vargas-Tendero, P., Paredes, M.D., Atucha, N.M. and García-Estañ, J. (2018) Flavonoids in kidney health and disease. *Front. Physiol.*, **9**, 394.

25. Malinowska, M., Wilkinson, F.L., Langford-Smith, K.J., Langford-Smith, A., Brown, J.R., Crawford, B.E., Vanier, M.T., Grynkiewicz, G., Wynn, R.F., Wraith, J.E., Wegrzyn, G. and Bigger, B.W. (2010) Genistein improves neuropathology and corrects behaviour in a mouse model of neurodegenerative metabolic disease. *PLoS One*, **5**, e14192.

26. Galarreta, C.I., Forbes, M.S., Thornhill, B.A., Antignac, C., Gubler, M.C., Nevo, N., Murphy, M.P. and Chevalier, R.L. (2015) The swan-neck lesion: proximal tubular adaptation to oxidative stress in nephropathic cystinosis. *Am. J. Physiol. Ren. Physiol.*, **308**, F1155–F1166.

27. Nevo, N., Chol, M., Bailleux, A., Kalatzis, V., Morisset, L., Devuyst, O., Gubler, M.-C. and Antignac, C. (2010) Renal phenotype of the cystinosis mouse model is dependent upon genetic background. *Nephrol. Dial. Transplant.*, **25**, 1059–1066.

28. Taranta, A., Elmonem, M.A., Bellomo, F., De Leo, E., Boenzi, S., Janssen, M.J., Jamalpoor, A., Cairoli, S., Pastore, A., De Stefanis, C. *et al.* (2021) Benefits and toxicity of disulfiram in preclinical models of nephropathic cystinosis. *Cell*, **10**, 3294.

29. Gaide Chevronnay, H.P., Janssens, V., Van Der Smissen, P., N'Kuli, F., Nevo, N., Guiot, Y., Levtchenko, E., Marbaix, E., Pierreux, C.E., Cherqui, S. *et al.* (2014) Time course of pathogenic and adaptation mechanisms in cystinotic mouse kidneys. *J. Am. Soc. Nephrol.*, **25**, 1256–1269.

30. Gaide Chevronnay, H.P., Janssens, V., Van Der Smissen, P., Liao, X.H., Abid, Y., Nevo, N., Antignac, C., Refetoff, S., Cherqui, S., Pierreux, C.E. *et al.* (2015) A mouse model suggests two mechanisms for thyroid alterations in infantile cystinosis: decreased thyroglobulin synthesis due to endoplasmic reticulum stress/unfolded protein response and impaired lysosomal processing. *Endocrinology*, **156**, 2349–2364.

31. Cheung, W.W., Cherqui, S., Ding, W., Esparza, M., Zhou, P., Shao, J., Lieber, R.L. and Mak, R.H. (2016) Muscle wasting and adipose tissue browning in infantile nephropathic cystinosis. *J. Cachexia. Sarcopenia Muscle*, **7**, 152–164.

32. Luciani, A., Festa, B.P., Chen, Z. and Devuyst, O. (2018) Defective autophagy degradation and abnormal tight junction-associated signaling drive epithelial dysfunction in cystinosis. *Autophagy*, **14**, 1157–1159.

33. Gaide Chevronnay, H.P., Janssens, V., Van Der Smissen, P., Rocca, C.J., Liao, X.H., Refetoff, S., Pierreux, C.E., Cherqui, S. and Courtoy, P.J. (2016) Hematopoietic stem cells transplantation can normalize thyroid function in a cystinosis mouse model. *Endocrinology*, **157**, 1363–1371.

34. Harrison, F., Yeagy, B.A., Rocca, C.J., Kohn, D.B., Salomon, D.R. and Cherqui, S. (2013) Hematopoietic stem cell gene therapy for the multisystemic lysosomal storage disorder cystinosis. *Mol. Ther.*, **21**, 433–444.

35. Syres, K., Harrison, F., Tadlock, M., Jester, J.V., Simpson, J., Roy, S., Salomon, D.R. and Cherqui, S. (2009) Successful treatment of the murine model of cystinosis using bone marrow cell transplantation. *Blood*, **114**, 2542–2552.

36. Sung, M.J., Kim, D.H., Jung, Y.J., Kang, K.P., Lee, A.S., Lee, S., Kim, W., Davaatseren, M., Hwang, J.T., Kim, H.J. *et al.* (2008) Genistein protects the kidney from cisplatin-induced injury. *Kidney Int.*, **74**, 1538–1547.

37. Abd El-Lateef, S.M., El-Sayed, E.S.M., Mansour, A.M. and Salama, S.A. (2019) The protective role of estrogen and its receptors in gentamicin-induced acute kidney injury in rats. *Life Sci.*, **239**, 117082.

38. Palanisamy, N. and Venkataraman, A.C. (2013) Beneficial effect of genistein on lowering blood pressure and kidney toxicity in fructose-fed hypertensive rats. *Br. J. Nutr.*, **109**, 1806–1812.

39. Ning, Y., Chen, J., Shi, Y., Song, N., Yu, X., Fang, Y. and Ding, X. (2020) Genistein ameliorates renal fibrosis through regulation snail via m6A RNA demethylase ALKBH5. *Front. Pharmacol.*, **11**, 579265.

40. Javanbakht, M.H., Sadria, R., Djalali, M., Derakhshanian, H., Hosseinzadeh, P., Zarei, M., Azizi, G., Sedaghat, R. and Mirshafiey, A. (2014) Soy protein and genistein improves renal antioxidant status in experimental nephrotic syndrome. *Nefrologia*, **34**, 483–490.

41. Zhang, J., Johnson, J.L., He, J., Napolitano, G., Ramadass, M., Rocca, C., Kiosses, W.B., Bucci, C., Xin, Q., Gavathiotis, E. *et al.* (2017) Cystinosin, the small GTPase Rab11, and the Rab7 effector RILP regulate intracellular trafficking of the chaperone-mediated autophagy receptor LAMP2A. *J. Biol. Chem.*, **292**, 10328–10346.

42. Nakamura, S., Shigeyama, S., Minami, S., Shima, T., Akayama, S., Matsuda, T., Esposito, A., Napolitano, G., Kuma, A., Namba-Hamano, T. *et al.* (2020) LC3 lipidation is essential for TFEB activation during the lysosomal damage response to kidney injury. *Nat. Cell Biol.*, **22**, 1252–1263.

43. Moskot, M., Montefusco, S., Jakóbkiewicz-Banecka, J., Mozolewski, P., Węgrzyn, A., Di Bernardo, D., Węgrzyn, G., Medina, D.L., Ballabio, A. and Gabig-Cimińska, M. (2014) The phytoestrogen genistein modulates lysosomal metabolism and transcription factor EB (TFEB) activation. *J. Biol. Chem.*, **289**, 17054–17069.

44. Chae, H.S., Xu, R., Won, J.Y., Chin, Y.W. and Yim, H. (2019) Molecular targets of genistein and its related flavonoids to exert anticancer effects. *Int. J. Mol. Sci.*, **20**, 2420.

45. Cherqui, S., Sevin, C., Hamard, G., Kalatzis, V., Sich, M., Pequignot, M.O., Gogat, K., Abitbol, M., Broyer, M., Gubler, M.-C. and Antignac, C. (2002) Intralysosomal cystine accumulation in mice lacking cystinosin, the protein defective in cystinosis. *Mol. Cell. Biol.*, **22**, 7622–7632.

46. Emma, F., Nesterova, G., Langman, C., Labbé, A., Cherqui, S., Goodyer, P., Janssen, M.C., Greco, M., Topaloglu, R., Elenberg, E. *et al.* (2014) Nephrophatic cystinosis: an international consensus document. *Nephrol. Dial. Transplant.*, **29**, iv87–iv94.

47. Ariceta, G., Giordano, V. and Santos, F. (2019) Effects of long-term cysteamine treatment in patients with cystinosis. *Pediatr. Nephrol.*, **34**, 571–578.

48. Battafarano, G., Rossi, M., Rega, L.R., Di Giovamberardino, G., Pastore, A., D'Agostini, M., Porzio, O., Nevo, N., Emma, F., Taranta,

A. *et al.* (2019) Intrinsic bone defects in cystinotic mice. *Am. J. Pathol.*, **189**, 1053–1064.

49. Mukund, V., Mukund, D., Sharma, V., Mannarapu, M. and Alam, A. (2017) Genistein: its role in metabolic diseases and cancer. *Crit. Rev. Oncol. Hematol.*, **119**, 13–22.

50. Lu, R., Zheng, Z., Yin, Y. and Jiang, Z. (2020) Genistein prevents bone loss in type 2 diabetic rats induced by streptozotocin. *Food Nutr. Res.*, **64**.

51. Bannwart, C., Fotsis, T., Heikkinen, R. and Adlercreutz, H. (1984) Identification of the isoflavonic phytoestrogen daidzein in human urine. *Clin. Chim. Acta*, **136**, 165–172.

52. Reda, A., Veys, K., Kadam, P., Taranta, A., Rega, L.R., Goffredo, B.M., Camps, C., Besouw, M., Cyr, D., Albersen, M. *et al.* (2021) Human and animal fertility studies in cystinosis reveal signs of obstructive azoospermia, an altered blood-testis barrier and a subtherapeutic effect of cysteamine in testis. *J. Inherit. Metab. Dis.*, **44**, 1393–1408.

53. Forbes, M.S., Thornhill, B.A., Galarreta, C.I., Minor, J.J., Gordon, K.A. and Chevalier, R.L. (2013) Chronic unilateral ureteral obstruction in the neonatal mouse delays maturation of both kidneys and leads to late formation of atubular glomeruli. *Am. J. Physiol. Ren. Physiol.*, **305**, F1736–F1746.

54. Bankhead, P., Loughrey, M.B., Fernández, J.A., Dombrowski, Y., McArt, D.G., Dunne, P.D., McQuaid, S., Gray, R.T., Murray, L.J., Coleman, H.G. *et al.* (2017) QuPath: open source software for digital pathology image analysis. *Sci. Rep.*, **7**, 16878.